www.lpr-journal.org

LASER & PHOTONICS REVIEWS

WILEY-VCH

LASER & PHOTONICS REVIEWS

Laser Photonics Rev. **5**, No. 3, 352–367 (2011) / **DOI** 10.1002/lpor.201000018

Abstract Electrons are among the lightest quantum particles in nature, yet they are of paramount importance in any kind of chemical reaction as they are the essence of molecular bonds. For several years, laser fields have been used towards the final goal of controlling chemical reaction dynamics. While early experiments focused mainly on the control of the internuclear wavefunction of rather heavy molecules, advances in short-pulse laser technology now allow the control of lighter molecules all the way down to hydrogen and even the direct control of electrons and their quantum wavefunctions. In this context, the stabilization and control of the carrier-envelope phase (CEP) of laser pulses has been one of the crucial technological advances that set off a revolution in ultrafast laser science. The authors review and summarize some of the past and current experimental achievements and theoretical ideas on CEP laser control of electrons. It will become clear that in some cases, depending on the control scenario, electrons can be considered to behave as classical particles and the control of their trajectories follow the laws of classical Newtonian mechanics while in other cases, the quantum nature of electrons is directly exploited to steer electron dynamics by means of quantum interference.

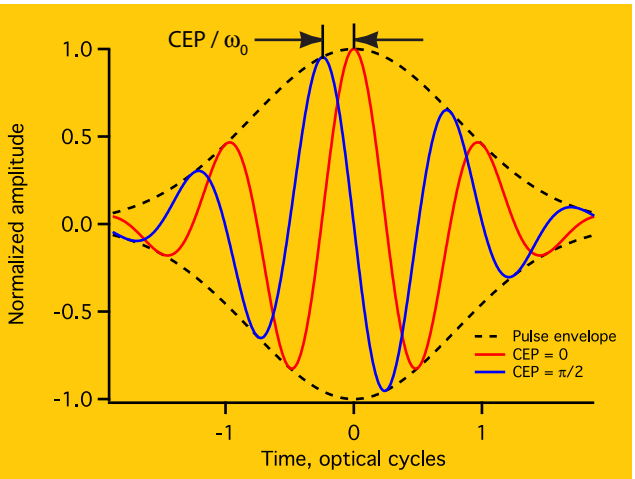

Classical and quantum control of electrons using the carrier-envelope phase of strong laser fields

Mark Abel [1,2,3,*], Daniel M. Neumark [1,2], Stephen R. Leone [1,2], and Thomas Pfeifer [1,2,4,*]

1. Introduction

The problem of how to guide a quantum system to a desired final state while avoiding unwanted states has fascinated the scientific community for a long time. Even before the quantum nature of matter was recognized, chemists were busy discovering ways to drive ensembles of atoms back and forth across the potential energy landscape making use of traditional chemical reactions performed by mixing gases, liquids and powders. The technically accessible control parameters were all thermodynamic: temperature, pressure, and concentration. Chemists had to contend with statistical thermodynamic averages, but soon after the invention of the laser the possibility of controlling the outcome of a chemical rearrangement using coherent light was born (for reviews see e. g. [1, 2]).

Generally, the coherent nature of the process is a key ingredient of quantum control. As phase relationships among quantum states are critical, the behavior of the driving fields on the dynamical timescale $h/\Delta E$ (with the Planck constant h and the maximum relevant quantum level spacing ΔE) of the system being controlled are important. The evolution of the electronic wavefunction among valence-level orbitals in atoms and molecules is characterized by an ultrashort timescale, typically a few femtoseconds or shorter. Therefore the femtosecond and even attosecond evolution of electric fields of light offers a powerful tool for quantum control and ultimately for control over the electron itself as the lightest chemically relevant quantum particle.

Two major experimental methods have evolved to gain direct access to sub-femtosecond phenomena: attosecond pulses and carrier-envelope-phase (CEP) controlled few-cycle electric fields at optical and infrared frequencies. In the latter, the electric *field evolution* (not just the *envelope*) of an ultrashort laser pulse can be controlled with sub-femtosecond precision. Attosecond pulse technologies and experiments have been summarized in a number of reviews to date (e. g. [3–5]). However, little emphasis has been devoted to obtaining a comprehensive picture of CEP control with lasers or to outlining the quantum-mechanical perspectives that can be addressed with such experiments. This is surprising, since CEP stabilization and control represent the ultimate theoretical limit of coherence given a certain number of photons and thus should provide the ideal tool for the exploration and further advance of coherent-control laser science.

Due to their perfect coherence, and thus fully defined phase, intense CEP-stabilized laser pulses allow one to study an exciting area of modern physics: the transition

[1] Departments of Chemistry and Physics, University of California, Berkeley, CA 94720, USA [2] Ultrafast X-ray Science Laboratory and Chemical Sciences Division, Lawrence Berkeley National Laboratory, Berkeley, CA 94720, USA [3] Fritz-Haber-Institut der Max-Planck-Gesellschaft, Faradayweg 4–6, 14195 Berlin, Germany [4] Max-Planck-Institut für Kernphysik, Saupfercheckweg 1, 69117 Heidelberg, Germany
[*] Corresponding authors: e-mail: markabel@fhi-berlin.mpg.de, tpfeifer@mpi-hd.mpg.de

between the quantum and the classical world. For quantum-mechanical transitions among states, the phase of the electric field plays a crucial role, and thus interference of many such transitions leads to well-known quantum-control processes where particular states can be selectively populated at the expense of others. However, due to the intense-field nature of the driving pulses, these multi-photon transitions very often involve the continuum as an intermediate (as in high-harmonic generation) or as a final state (as in above-threshold ionization). In this case, the action accumulated by the electron along its quantum path can become extremely large, sometimes leaving just one stationary-phase quantum path: the classical trajectory of the electron. Again, the CEP proves an ideal parameter to control the motion of quantum particles close to this classical limit.

This review article focuses on the ways and physical pictures in which the CEP of few-cycle pulses can be used to control the dynamics of electrons in atoms and molecules. The CEP plays a key role in a diverse array of processes ranging from the selective excitation of one state in a degenerate manifold to the generation of isolated attosecond pulses. As mentioned above, the main focus of this review article is on the distinction between quantum control and classical control of electrons and the fascinating transitions between the classical and the quantum regime illuminated by fully-coherent CEP-controlled light fields.

2. Stabilization and control of the CEP

For laser pulses consisting of only a few optical cycles, the phase offset of the carrier with respect to the envelope, the CEP, influences significantly the shape of the electric field under the pulse amplitude envelope. This situation is illustrated in Fig. 1, where the electric field and envelope function of a few-cycle optical pulse are plotted. One can thus easily imagine that the CEP can influence the outcome of such few-cycle pulses' interaction with matter. A CEP of zero means that the two extrema of carrier and pulse envelope are perfectly synchronized to yield a so-called cosine pulse, and a CEP of $\pi/2$ means that the maximum of the wave is a quarter cycle displaced from the pulse amplitude maximum in time, yielding a sine-like pulse. When the CEP is π, the original cosine pulse is simply inverted in the laboratory frame of reference (the pulse is multiplied by the phase factor $e^{-i\pi} = -1$).

In the time domain, the role of the CEP is determined by the behavior of a laser pulse propagating in a laser cavity [6]. For mode-locked lasers emitting a train of short pulses, the spectrum consists of a comb of narrow spikes, separated by the repetition rate of the laser. As a result of the mismatch between group and phase velocities of the pulse in the laser cavity, the pulse in general suffers a non-zero phase shift as it makes a round trip through the cavity. When considering the output spectrum of the laser, then, this phase shift over the round trip through the cavity corresponds to a frequency: the carrier-envelope offset frequency (CEO frequency). Returning to the time-domain, consider that each pulse emitted from the laser oscillator will have a small phase shift relative

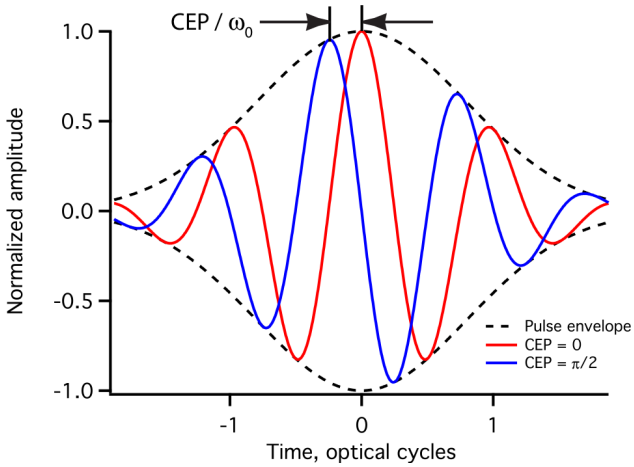

Figure 1 (online color at: www.lpr-journal.org) The carrier envelope phase is the temporal offset between the maxima of the carrier wave and the pulse envelope, converted to a phase using the carrier frequency. The time-symmetric electric field has CEP $= 0$, and the time-antisymmetric field has CEP $= \pi/2$. Because the pulse is few-cycle in nature, the CEP strongly affects the shape of the wave under the amplitude envelope.

to the preceding one: the CEP changes from pulse to pulse. This shift is the phase slip over one cavity round trip, or equivalently 2π times the ratio of the CEO frequency to the repetition rate. Therefore, a CEP-stable laser is one for which the CEO frequency is zero: the CEP is the same for every pulse emitted.

Carrier-envelope phase stabilization techniques [7–15] allow experimental control over this important parameter. In the spectral domain, the CEP manifests itself as a spectral phase term (a constant) in addition to a possible chirp of a laser pulse. As such, it is one of the terms in the commonly-employed Taylor series expansion of the spectral phase that, along with the spectral amplitude, determines the time-dependent electric field. As the CEP acts globally on the spectral phase (by shifting the entire spectral phase function up or down), it is ultimately important to define a fully spectrally coherent laser pulse.

To briefly explain a widely-used CEP stabilization scheme, consider the effect of the CEP in nonlinear-optical frequency doubling, simply using one chirped laser pulse. To observe effects that depend on the CEP, we need a single laser pulse that contains both frequencies, ω and 2ω in its spectrum – i. e. the spectrum needs to cover an optical octave. Then the fundamental and its second harmonic overlap in frequency and will result in a spectral interference pattern observed on a spectrometer (see Fig. 2). The measured fringe pattern in the spectral overlap region then encodes the phase difference between the two pulses, including the CEP. By taking explicit account of the CEP in the temporal phase, the complex light field $E_{\mathrm{tr}}(\omega)$ transmitted through a frequency-doubling crystal can be approximately constructed as the sum of the input and frequency-doubled

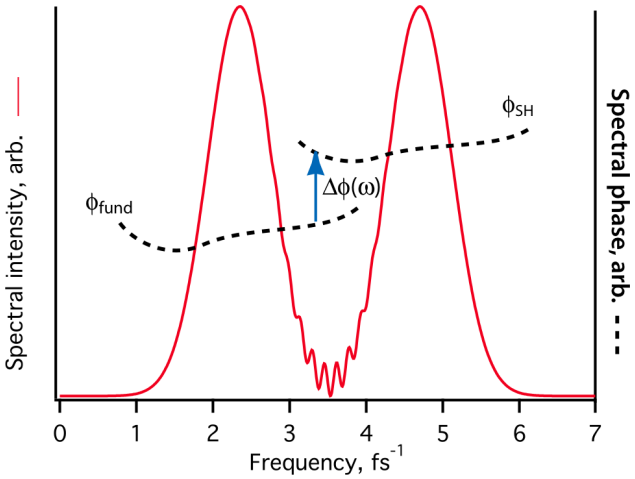

Figure 2 (online color at: www.lpr-journal.org) Calculated output of an f-$2f$ interferometer. An ultrashort pulse with spectrum centered at 2.35 fs^{-1} and phase ϕ_{fund} is frequency doubled in a nonlinear crystal, spectrally overlapping its own second harmonic (center frequency 4.7 fs^{-1}, spectral phase ϕ_{SH}). The combined spectrum contains interference fringes that encode the phase difference, including the CEP.

fields with spectral envelopes ε and $\varepsilon^{(2)}$:

$$E_{\text{tr}}(\omega) \sim e^{-i\phi_{\text{CEP}}}\varepsilon(\omega)e^{-i(\phi_{\text{GDD}}(\omega)+\phi_{\text{TOD}}(\omega)+\ldots)} + a(\omega)e^{-2i\phi_{\text{CEP}}}\varepsilon^{(2)}(\omega)e^{-i\left(\phi^{(2)}_{\text{GDD}}(\omega)+\phi^{(2)}_{\text{TOD}}(\omega)+\ldots\right)}. \quad (1)$$

Here, $a(\omega)$ is the frequency-dependent doubling efficiency, containing the effective nonlinearity, phase matching effects, etc. The group delay dispersion (GDD) and third order dispersion (TOD) phase terms are explicitly counted. Because the phase at every frequency has a contribution $e^{-i\phi_{\text{CEP}}}$, any pair of frequencies from the fundamental pulse that combine will generate a second harmonic field with a phase contribution $e^{-2i\phi_{\text{CEP}}}$. The remainder of the spectral phase is determined by the autoconvolution of the input field. Therefore the second term, caused by the frequency-doubled light, is out of phase with the first term by the CEP, plus a contribution from the remainder of the spectral phase. In principle, detailed knowledge of the spectral (or, equivalently, temporal) phase of the input laser pulse is enough to retrieve the absolute value of the CEP from the f-$2f$ interferogram. However, the accurate characterization of octave-spanning laser pulses is extremely difficult and comprises a research field in itself. As a result, f-$2f$ interferometry is generally only used to detect relative changes in the CEP for use as the input to a feedback loop.

This CEP stabilization method is called an f-$2f$ interferometer and is useful for stabilizing the CEP of high-power amplified lasers [10, 16]. The frequency-comb stabilization techniques pioneered even earlier by Hänsch and Hall [17] for high-repetition-rate laser systems are also related to this f-$2f$ interferometry principle. For additional reviews on CEP-stabilization and frequency-comb techniques, see e. g. [18, 19]

Roughly speaking, the "octave-wide spectrum" condition is fulfilled when the pulse is "few-cycle" in nature: the duration τ is comparable to the carrier wave period T. In this case the envelope is comparable in duration to the period of the carrier wave and the field changes significantly in field strength between extrema of the carrier (Figure 1). In a few-cycle pulse the width of the spectrum becomes comparable to the center frequency and thus typically the octave-wide spectrum is obtained.

Alternatively, one could interfere frequency-doubled (generally, n-tupled) with frequency-tripled (or generally $(n+1)$-tupled) light. This approach requires only frequencies ω and $[n/(n+1)]\omega$ to be contained in the spectrum of the laser pulse, which eases the requirements on the required bandwidth as n becomes larger. Therefore one could still expect to observe CEP effects in the case of longer "multicycle" driver laser pulses in an experiment. Also, intra-pulse difference-frequency mixing and interference with the fundamental light has been successfully employed for CEP detection and stabilization [20]. A recently-explored technique used direct electro-optical radio frequency subtraction of the CEP-offset-frequency from an oscillator pulse train by an acousto-optic modulator to control the CEP [15].

3. CEP quantum control of electrons

Several methods have been explored for controlling quantum dynamics. For example, one can take advantage of the molecular potential-energy surfaces of excited electronic states in combination with sequences of two or more time-delayed laser pulses to guide molecules to the desired reaction pathway (the Tannor-Kosloff-Rice scheme [21, 22]), or transfer population coherently from one quantum state to another with unit probability by using suitably tailored adiabatic light fields (the stimulated Raman adiabatic passage, or STIRAP, scheme [23]). Interfering multiphoton transitions pumped at different frequencies was another approach to coherent control with lasers (Brumer-Shapiro scheme [24]), the one perhaps most relevant to CEP-based control.

The Brumer-Shapiro phase control scheme begins by noting that when a quantum system like an atom or a molecule is perturbed by a laser pulse it can make a transition from an initial state $|i\rangle$ to another final state $|f\rangle$ that is dipole allowed with a dipole matrix element $\vec{\mu}_{if}$. The transition probability p right after the interaction with a short pulse (much shorter than the lifetime of the final state) is given as the square of a complex transition amplitude for a field at frequency ω_r, corresponding to the transition energy $\hbar\omega_r$:

$$p \propto \left|\langle f|\vec{\mu}\cdot\vec{E}(\omega_r)|i\rangle\right|^2 \quad (2)$$

In the rotating wave approximation, $\vec{E}(\omega) = \vec{\varepsilon}(\omega)\exp(-i\phi(\omega))$ is complex. It is composed of the spectral amplitude $\varepsilon(\omega)$ and spectral phase $\phi(\omega)$. As can be seen in the above equation, the phase of $E(\omega_r)$ drops out of the transition probability in this linear process, and thus it cannot be used to control the transition probability. Only the

spectral amplitude of the laser pulse would govern the transition probability and as such, there would be, in this linear regime, no means of controlling the transition probability to different energetically degenerate states, as their relative transition probabilities would be given by their relative dipole moments only.

Quantum-mechanical phase control requires the coherent addition of multiple quantum paths, each with a different phase. This is an old principle of quantum mechanics, well-known since the time of the first double-slit experiments. Brumer and Shapiro extended this principle to multiple nonlinear-optical transitions with the explicit goal of controlling population transfer [25, 26]. They considered the interference between one quantum path involving absorption of a photon, and a second path involving the absorption of *three* photons at three times the wavelength. Three, not two, photons are chosen for the second path so that both are parity-allowed. Then the amplitudes for transitions involving each of the two waves add, and the probability is the coherent sum:

$$p \propto |\varepsilon(3\omega)e^{-i\phi(3\omega)}\mu_{if} + (\varepsilon(\omega)e^{-i\phi(\omega)})^3\chi_{if}|^2, \quad (3)$$

where χ_{if} is a transition hyperpolarizability matrix element. In this case, there is an explicit dependence on the relative phase $\phi(3\omega) - 3\phi(\omega)$ in the transition probability. This situation is represented in Fig. 3. The above-discussed f-$2f$ method for measurement and stabilization of the CEP by nonlinear-optical means is, at its heart, also an example of Brumer-Shapiro control. It demonstrates nicely the utility of the CEP: Brumer-Shapiro-style control can be achieved *within a single laser pulse* with fully determined spectral phase.

Equation (3) also reveals why such intra-pulse Brumer-Shapiro control cannot be achieved when averaging the response of a quantum system over multiple pulses from a CEP-unstable laser. Forgetting the details of dipole moments and field vectors, Eq. (3) has the form

$$p(\phi) \propto \left|C(n\omega)e^{-i\phi_{\mathrm{CEP}}} + D(\omega)e^{-in\phi_{\mathrm{CEP}}}\right|^2 \quad (4)$$

with n an integer (in the case of using a single laser pulse to make the transitions in Fig. 3, $n = 3$). Here, the spectral

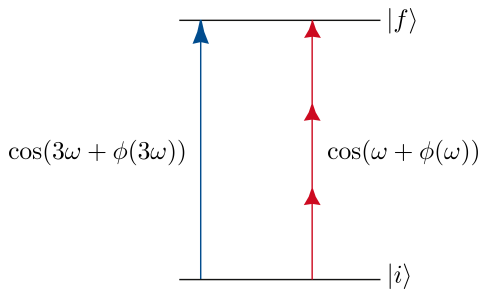

Figure 3 (online color at: www.lpr-journal.org) The Brumer-Shapiro quantum control scheme utilizes two colors of light, with different phase. When two levels are coupled by one photon of the blue wavelength and three photons of the red wavelength (to satisfy the parity selection rule), the phase difference between the two beams determines the population transfer.

phase apart from the CEP is absorbed into the transition matrix elements C and D. Averaging p over ϕ_{CEP} yields

$$\langle p\rangle_\phi \propto \left\langle |C|^2 + |D|^2 + C^* D e^{-i(n-1)\phi_{\mathrm{CEP}}} + CD^* e^{i(n-1)\phi_{\mathrm{CEP}}} \right\rangle . \quad (5)$$

But since $\langle e^{in\phi}\rangle = \langle e^{-in\phi}\rangle = 0$, the average reduces to the incoherent sum of the two pathways. When using CEP-unstable lasers, CEP effects have to be investigated using coincidence methods, working one laser pulse at a time [27, 61]. Traditional Brumer-Shapiro control experiments used frequency-n-tupled light ($\phi(n\omega) \sim n\phi(\omega)$) derived from the same CEP-unstable fundamental pulse. In that case, the CEP dependence drops out of the transition probability, which is not the case for the intra-pulse Brumer-Shapiro control described here.

Some theoretical work on CEP-based control has focused on this type of multi-path quantum interference. For example, Nakajima and Watanabe [28, 29] calculated the response of bound-level populations in atoms by solving the time-dependent Schrödinger equation for relatively weak few-cycle pulses. These pulses were strong enough to excite multiphoton transitions, but the ponderomotive potential was much less than the ionization potential. They found a strong CEP dependence of the level populations even though the total ionization yield was insensitive to CEP.

In that case, the authors discussed their results in terms of a three-level system. They argued that in second-order perturbation theory the result for the final state population contained a non-negligible CEP-dependence in the case of short driving pulses. But in view of the Brumer-Shapiro model presented above, one would expect that a two-level system should also show CEP-dependence in the transition probability when excited by a few-cycle pulse.

Actually, similar experiments were being carried out at around the same time as Nakajima and Watanabe were doing their calculations. Fortier et. al. [30, 31] irradiated GaAs with few-cycle pulses resonant with the band-gap transition and monitored the photocurrent as a function of CEP. In this experiment, the photocurrent varies sinusoidally with CEP, first flowing one direction then the other as the CEP is scanned. This experiment is a little different than the atom work, because the measured result is not the population of a single state but rather the population imbalance between two degenerate states. Similar phase-sensitive semiconductor experiments were also performed a decade earlier, using two phase-locked laser sources [32].

In the continuum (either the vacuum or the conduction band of a crystal), the electron wavefunction is specified by a wavevector. At a particular momentum, $|\vec{k}\rangle \sim e^{i\vec{k}\cdot\vec{x}}$ and $|-\vec{k}\rangle \sim e^{-i\vec{k}\cdot\vec{x}}$ are degenerate. We can write linear combinations of $|\vec{k}\rangle$ and $|-\vec{k}\rangle$ that have definite parity. They are:

$$|\pi+\rangle = \frac{1}{\sqrt{2}}\left\{|\vec{k}\rangle + |-\vec{k}\rangle\right\} \quad (6)$$

and

$$|\pi-\rangle = \frac{1}{\sqrt{2}}\left\{|\vec{k}\rangle - |-\vec{k}\rangle\right\} . \quad (7)$$

Now, excitation from an even-parity ground state (for example) by one photon leaves population in the odd-parity final state $|\pi-\rangle$. Excitation from an even-parity ground state by *two* photons of half the energy transfers population to the even-parity final state $|\pi+\rangle$. Since the photons were coherent, so is the final state: a superposition of $|\pi+\rangle$ and $|\pi-\rangle$. This superposition will – in general – have different weights for electrons traveling one direction and the other. Control over the electron direction in semiconductor photocurrent experiments – and the results of Nakajima and Watanabe's TDSE solution – is nothing other than multiple quantum-path interference.

All this can be summed up nicely by the theoretical work of Roudnev and Esry [33]. They separated the time-dependence of the carrier wave (which includes the CEP) from the time dependence of the envelope by employing two time variables. This allows a neat rearrangement of the Schrödinger equation so that the wavefunction can be re-written in the Floquet representation. This representation is nothing more than splitting each single atomic state into multiple states, with each new state having a different number of photons in the laser field. Then, transitions between levels having different atomic origins and different photon numbers can be calculated using the language of avoided crossings [34].

The benefit of octave spanning, few-cycle pulses for control is that the multiple-order quantum-path interference can be achieved within a single pulse, with the relative phase between the pathways determined by the CEP. This scheme offers the possibility of directly controlling electrons in bound levels of atoms and molecules on the timescale of the lightwave.

4. CEP control of electron localization in molecules

A recent focus of quantum-mechanical CEP control is the localization of the electronic wavefunction during dissociative ionization of diatomic molecules. The subject of diatomic molecules in strong laser fields is rich, with many effects like bond softening, enhanced ionization, recollision excitation and ionization, and sequential excitation and ionization all potentially resulting from the molecule-laser interaction [35]. We focus here on some recent experimental results on electron localization.

The first efforts to understand CEP effects in molecule-strong-laser interactions were theoretical. Numerical solution of the time-dependent Schrödinger equation for HD^+ dissociation was carried out in 2004 [36]. The result suggested that imaging the reaction products was necessary to observe a strong CEP-dependence on the electron localization (H^+ or D^+ production). Around the same time, Bandrauk et al. [37] calculated the electron localization in the case of a VUV-pump, VUV-probe experiment. The asymmetry in the electron distribution was the result of the coherent excitation of the $2p\sigma_u$ state of the molecular ion, however, and not due to CEP effects. Experiments were soon to follow with the publication of the experimental work of Kling et al. in 2006 [38]. There the authors used a single, intense, CEP-controlled wave to both ionize and dissociate D_2. The direction of ion emission was always maximal along the laser polarization direction, and the ion asymmetry (number going parallel vs. antiparallel to the laser field) varied sinusoidally with CEP over a broad range of ion kinetic energies. The experimental dissociative ionization results were explained qualitatively in the following way. Ionization of D_2 is assumed to occur in a narrow temporal window at the peak of the pulse. The free electron returns to the ion half a cycle later and collides, exciting the ion to the $2p\sigma_u^+$ state. This state is strongly repulsive, so the molecule starts to break apart. As it dissociates, the laser field continues to interact with it, generating a coherent superposition of ground (gerade) and excited (ungerade) states; this therefore establishes a time-dependent electron localization. This oscillation of electron density eventually ceases as the nuclei get far enough apart that the oscillation period becomes very large in time or the coherence of the electronic wavefunction is destroyed (incidentally, such superpositions can be quite long-lived [39, 40]).

The Kling results are represented in Fig. 4, where the ionization of D_2 and subsequent excitation of the ion are shown. Their calculation of time-dependent populations and electron localization parameter are also shown.

One might have expected some CEP dependence of the ionization rate (since the intensity was 10^{14} W/cm^2) [41,42], but the authors did not consider it. In a subsequent experiment in H_2, no correlation between the ionization step and the electron localization was found [43]. On the contrary, in the case of carbon monoxide, a similar experiment was performed and the asymmetry was calculated to come 75% from the ionization step [44]. The remaining 25% was attributed to the laser-induced population transfer and resulting coherent dynamics between electronic levels.

Vrakking's group also performed an experiment on H_2 using attosecond pulses rather than field ionization [45, 46], as illustrated in Fig. 5. They also found that asymmetry is caused by laser-coupling of ionic potential curves. In these experiments, the dissociating nuclear wavefunctions move on dressed curves that are eigenstates of the molecular two-level system in the presence of a coupling laser field. At close internuclear spacing, the energy gap between the states is larger than the laser-induced coupling and the eigenstates are virtually unchanged. At larger separations, the energy gap between the two molecular eigenstates becomes close to the laser frequency and the coupling becomes large. Now the correct eigenstates are those field-dressed states that diagonalize the two-level Hamiltonian with laser-coupling included. Thus a coherence is established between the molecular states and the electron is strongly polarized by the laser field, first localized on one nucleus then on the other as the field changes direction. As the nuclei continue to move apart, the two electronic levels move out of resonance again and the polarization stops changing sign.

The population is determined in the Landau-Zener model (and first-order perturbation theory within the rotating-wave approximation) by the field envelope while the polarization (relative phase) of the states is determined

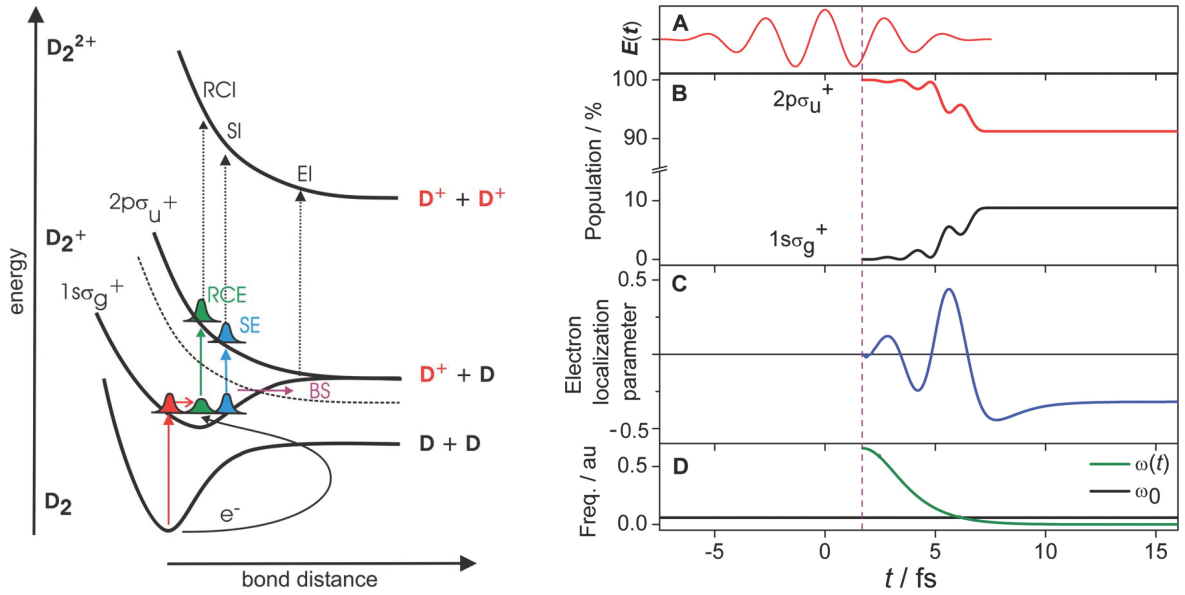

Figure 4 (online color at: www.lpr-journal.org) Dissociative ionization of D_2. Figure from [38]. Left panel: After ionization by a strong visible laser field $E(t)$ to the D_2^+ ground state (red arrow), the free electron can re-collide with the ion exciting it to the repulsive curve (RCE, green arrow) or the ion can be excited by the laser field in sequential excitation (SE, blue arrow). D^+ can also be generated by recollision ionization (RCI), sequential ionization (SI), bond softening (BS), or enhanced ionization (EI). (For more information see [38].) Coherence and interference created between the two levels by the laser pulse lead to electron localization on one or the other nucleus. Right panel: laser field (A), calculated population in the two levels of D_2^+ (B), calculated electron localization (C), and calculated eigenfrequency of the system $\omega(t)$ (ω as a function of t, as appears in Fig. 4D) compared to the laser frequency ω_0 (D).

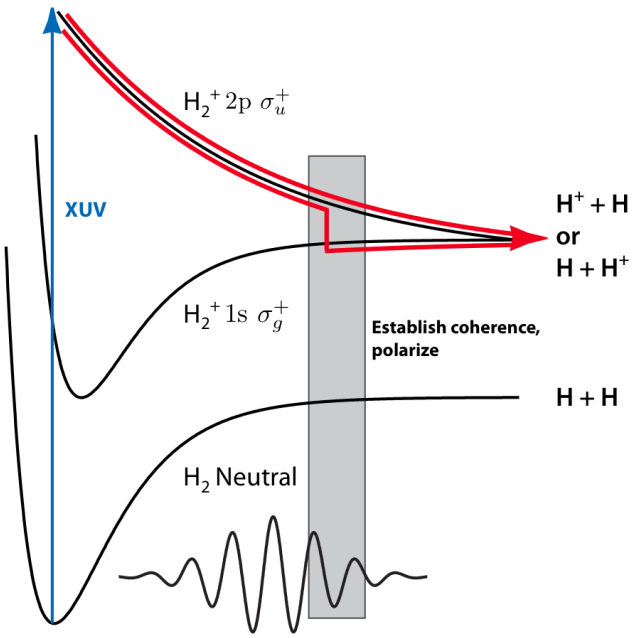

Figure 5 (online color at: www.lpr-journal.org) Control of electron localization in dissociative ionization. After ionization to the repulsive $2p\sigma_u^+$ state of H_2^+, the ion evolves through an internuclear separation where a visible laser pulse causes coupling between the two ion states (shaded gray area). Population is transferred to the $2p\sigma_u^+$ curve with a phase offset depending on the CEP. The resulting electron localization is detected as in Fig. 4.

by the phase of the field oscillations and hence by the CEP. Thus the CEP tunes the relative phase of the final superposition of $2p\sigma_u^+$ and $1s\sigma_g^+$. When the atoms separate enough that the electron can no longer move freely from one nucleus to the other, the oscillation is frozen and the electron becomes permanently localized.

This case is different and slightly more complicated than the "pure" Brumer-Shapiro cases of the f–$2f$ interferometer, the semiconductor photocurrent experiments, and the excitation probabilities of Nakajima and Watanabe. Here, one has evolution of the molecular wavefunction on two separate electronic surfaces and the system continues to undergo nontrivial dynamics after the laser pulse is over. Despite the differences in detail however, one must acknowledge that at their heart these localization experiments on molecules are another demonstration of localization by multi-path quantum interference.

5. CEP control at the quantum-classical transition in strong-field ionization

The simplicity of this multiple quantum-path idea is appealing, but one has to ask, is it still useful for large laser field strengths [47]? In strong-field ionization of atoms and molecules, an electron typically undergoes multi-photon or tunnel ionization; both are quantum-mechanical in nature. But as soon as the electron becomes unbound, it distributes its wavefunction across a continuum of states. Can we "quantum control" electronic motion in the continuum?

A strong-field ionized electron is further accelerated by the laser field and can finally be measured when impinging on a detector [48–50]. This "above-threshold ionization" (ATI) – so called because the electrons may acquire far more kinetic energy than one photon's worth – is also finely controlled by the CEP [27, 51–53].

Multiple-path interference is by no means restricted to one- and two-photon pathways, as pointed out already by Brumer and Shapiro [24]. In this context, the Berkeley group has carried out an experiment where e. g. nine- and ten-photon pathways interfered in the ionization of Xe atoms with a few-cycle laser pulse [54]. We observed the same type of CEP-dependence, even at high driving field strengths approaching the regime where tunneling ionization becomes important. We explored the behavior of quantum-mechanical control in the intermediate region between multi-photon and strong-field regimes [54].

In the case of [54], the intensity of the laser used to ionize Xe atoms was just enough to generate a few peaks in the photoelectron spectrum, separated by the laser photon energy. The phase of the electron wavepackets comprising each peak was determined by the phase of the laser pulse, including its CEP. The CEP enters in a similar way as discussed in the case of the f-$2f$ interferometer and the experiments with one- and two-photon transitions across the bandgap in semiconductors: the neighboring peaks in our photoelectron spectrum – exhibiting pairwise opposite parity – overlap and interfere, with phase difference equal to the CEP plus a contribution due to higher-order contributions to the spectral phase. It is thus possible to use the CEP for controlling the asymmetry of electron emission at kinetic energies just in between neighboring ATI peaks, as can be seen in Fig. 6b. A characteristic periodicity of the observed asymmetry patterns is visible as a function of photoelectron energy, corresponding to features repeating at exactly one photon energy – the spacings of the ATI peaks. At higher kinetic energies, this distinct quantum interference pattern gives way to a more continuous structure, pointing at a different control mechanism which will become clear in the following.

Up to now we have discussed in detail the control of electron wavefunctions in the weak-field limit, where it is seen that the population in the final state of interest is given by the coherent sum of all quantum pathways from the initial state, each pathway with an associated phase. One can consider the sum over quantum pathways as a sum over possible emission and absorption events, where the n-photon absorption pathway is given by a sum of absorption of n photons, absorption of $n+1$ photons and emission of 1 photon, etc. One also has to take into account the variety of wavelengths available from the laser pulse so that the n-photon pathway is really a sum over combinations of colors that result in the final electron energy under consideration. In the classical limit, the interaction with the field is so strong that many different pathways involving many absorption and emission events become likely. Thus the discrete nature of the ATI spectrum begins to be washed out and the classical trajectories of the electrons in the field become relevant.

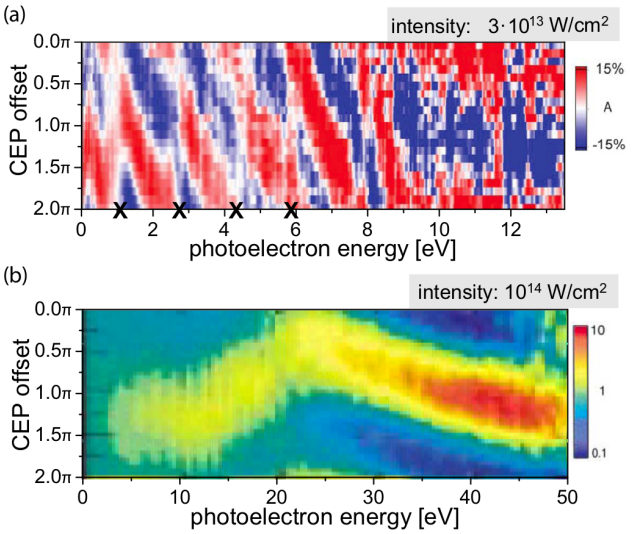

Figure 6 (online color at: www.lpr-journal.org) Quantum-classical transition observable in above-threshold ionization (ATI). Experimental ATI asymmetry maps at different laser intensities show remarkably different structure. **(a)** At lower field strengths, only lowest-order multiphoton amplitudes contribute significantly to the ionization amplitude [54]. The asymmetry changes as a function of energy with a periodicity corresponding to the photon energy, and is largest in between ATI peaks, where interference between transitions involving n and $n+1$ photons occurs. Positions of peaks in the corresponding photoelectron spectra are marked with X. **(b)** At high field strengths, the photoelectrons follow classical trajectories and the asymmetry has a smooth energy-dependence [55]. In both panels the color scale represents asymmetry, with red being more electrons going up in the lab frame. Note, however, the different definitions of asymmetry: in [54] $a = (n_{\mathrm{up}} - n_{\mathrm{down}})/(n_{\mathrm{up}} + n_{\mathrm{down}})$, while in [55] $a = n_{\mathrm{up}}/n_{\mathrm{down}}$. The scale of the asymmetry is also different: a is some 15% in panel (a), while more than a factor of 10 (corresponding to nearly 90% using the definition of [54]) in panel (b).

This transition is illustrated in Fig. 6 where the experimental asymmetry of ATI electron emission in CEP-stabilized laser pulses is displayed for two cases: the classical regime [55] where the electron absorbs and emits many photons, and the quantum regime [54] where the electron absorbs just enough photons to get to the final state. Interestingly, it may be that there is an onset of classical behavior in the latter case, where the periodic structures in the asymmetry plot give way to smooth variation near 10 eV photon energy. This transition is also observed in [56], although the authors focused on the high-energy electrons and did not comment on the low-energy electrons. Note that scalings other than intensity can be used to transition between quantum and classical regimes. For example, Colosimo and co-workers used the wavelength of the ionizing laser to make the transition [57].

To understand the CEP dependence of the classical version of the ATI process, let us consider a simple quasi-classical model that ignores electron phases. The ionization rate as a function of time $\Gamma(t)$ depends on the laser field according to the well-accepted Ammosov-Delone-Krainov

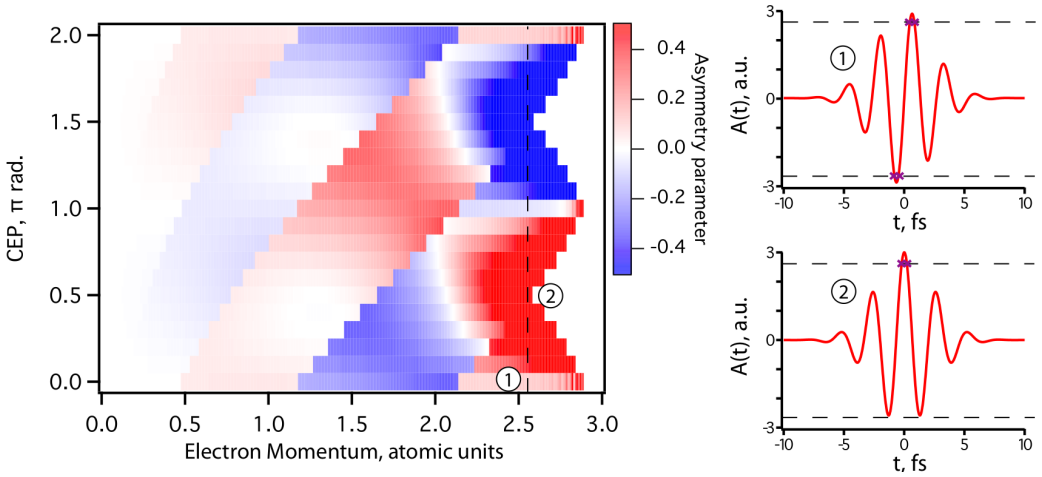

Figure 7 (online color at: www.lpr-journal.org) Asymmetry parameter for model discussed in text. The asymmetry is computed for a 5.7 fs, vertically polarized laser field of 800 nm wavelength, with peak vector potential 3 atomic units. Note the horizontal scale is momentum, not energy. Positive asymmetry means more electrons go up in the laboratory frame. When the CEP of the laser field is near zero in case (1) the asymmetry is very small, while for a CEP $\approx \pi/2$ in case (2) the asymmetry is large because the vector potential only crosses the associated value during one half cycle.

(ADK) formula [41]. According to the streak-camera principle [58, 59], the final momentum of the electron released at time t_r is just given by the negative vector potential at the time of release, $p(t_r) = -A(t_r)$, and $A(t)$ is the indefinite integral of the field $E(t)$ multiplied by the speed of light c. Putting these together, we can make a simple 1-dimensional model of the emission spectrum. One simply has to integrate over all times, asking at each time, how many electrons are released and whether they will end up with the desired momentum (neglecting any interactions with the ion or interferences):

$$N(p) = \int_{-\infty}^{\infty} \Gamma(t)\,\delta(-A(t) - p)\,dt \tag{8}$$

$$= \int_{-\infty}^{\infty} \Gamma(t) \sum_{t^*} \frac{\delta(t - t^*)}{|-dA/dt|_{t^*}|}\,dt \tag{9}$$

$$= \sum_{t^*} \frac{\Gamma(t^*)}{|cE(t^*)|} \tag{10}$$

where t^* are the solutions of $A(t) + p = 0$. We see that the emission into momentum state $|p\rangle$ is determined by the ionization rate at a few distinct points in time, when $A = -p$, and the electric field at these times. Suppose we have a Gaussian pulse. Using the above equation it is straightforward to compute the emission spectrum and the momentum-dependent asymmetry parameter

$$a(p) = \frac{N(p) - N(-p)}{N(p) + N(-p)}. \tag{11}$$

The calculation was performed for a 5.7 fs electric field (4 fs intensity profile) at 800 nm carrier frequency and peak vector potential of 3 atomic units acting on an atom with ionization potential $I_p = 1/2$ atomic unit (13.6 eV). For simplicity the ionization rate was calculated as $\Gamma(t) = \exp(-4\sqrt{2}I_p^{3/2}/3E(t))$, which leaves off the prefactors from the ADK expression. The calculated asymmetry as a function of photoelectron momentum and CEP is shown in Fig. 7. As the CEP changes, the asymmetry changes sign for fixed momentum. One also notices that at fixed CEP, the asymmetry as a function of electron momentum varies about zero – first it might be positive, then it swings negative, only to change sign again. Each of these sign changes corresponds to a momentum where another half cycle of the vector potential is no longer able to contribute electrons at the requisite momentum. For the combinations of momentum and CEP where many half-cycles contribute, the asymmetry is small. If only one half-cycle contributes, the electrons all go in one direction determined by the CEP.

One can see that the asymmetry as a function of momentum is a unique function of CEP, and therefore the CEP can be determined in principle from the ATI spectrum. This has been achieved experimentally, and it can be used to lock the CEP against slow drifts [52, 53, 55, 60, 61]. While the low-energy portion of the ATI spectrum contains some CEP-dependent asymmetry, there is a much larger asymmetry in the final directions of electrons that scatter elastically off their parent ions. These electrons can be accelerated in the field to many times the ponderomotive energy and give rise to a high-energy tail in the ATI spectrum. They are extremely sensitive to the CEP – again through their classical trajectories as determined by the laser field – and thus provide an ideal signal for absolute CEP determination and for CEP stabilization. This fact is illustrated in Fig. 8, where the ATI spectra of a few-cycle laser pulse are used to determine the CEP unambiguously.

The CEP is not the only physical quantity that can be retrieved from ATI momentum distributions. In fact, many more complicated effects than just those described above play a role in the ionization process. For example, other laser pulse parameters like duration and intensity, as well

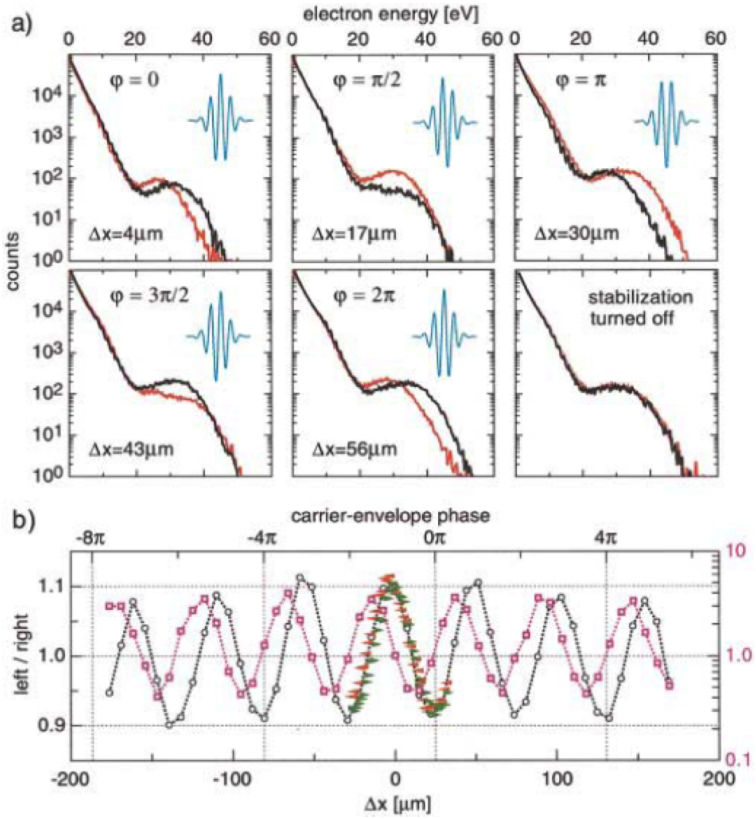

Figure 8 (online color at: www.lpr-journal.org) Phase meter based on ATI. The asymmetry of electron emission in a few-cycle laser field was used in [55] to determine and stabilize the absolute phase. Plots in (a) show the electron spectra in the leftward (black) and rightward (grey, red online) directions for various values of the CEP, controlled by inserting a glass wedge into the laser beam. Plot (b) shows the asymmetry as a function of glass wedge insertion distance (or equivalently, CEP). Circles are for low energy electrons (energy less than 20 eV) and squares are for high energy electrons (energy greater than 20 eV). Note the different vertical scales for the two curves.

as structural information about the target, can be obtained from ATI experiments [62–64]. Nor is our mathematical analysis by any means state-of-the-art. Readers interested in more detailed models of above-threshold ionization that can be extended to include scattering, interference effects, etc. should see the excellent reviews in [65–67].

A similar idea to the above analysis has been discussed for the case of nanoparticles [4,68]. In nanoparticles, a weak light field resonant with the surface plasmon frequency can induce an enormous dipole oscillation of conduction band electrons across the particle. The fields generated by the plasmon are generally several orders of magnitude stronger than the input light field. This enhanced field can accelerate electrons released from the nanoparticle during the lifetime of the plasmon resonance. Clearly, with minimal changes to the ionization rate $\Gamma(t)$, the above model will also qualitatively describe CEP-dependent photoemission from nanoparticles.

This formulation is qualitative, of course, but it has been put on firmer footing by the extensive recent research into high-harmonic generation, a strong-field phenomenon closely related to ATI.

6. Classical CEP control and high-harmonic generation

In high-harmonic generation (HHG), visible laser light is converted to extreme-ultraviolet (XUV) wavelengths by means of a nonlinear interaction in a gas. In the very beginning of high-harmonic investigations, it was proved that a perturbative approach, going to ever higher orders in perturbation theory, would never converge to give the proper description of HHG [69,70]. The process at work was found by a radical new approach to the problem: an electron that performs a classical closed-loop trajectory in the continuum starting from, and returning to, its parent atom.

In HHG, an electron in a valence level of an atom tunnels out of the binding potential under the influence of the laser field. It is accelerated by the laser field and can eventually recombine, releasing its kinetic energy as a high-energy photon [50, 78]. HHG is important for many reasons, including the possibility of using it to generate sub-fs XUV pulses [4, 59, 71–75]. The CEP of the driving laser pulse in HHG has a strong effect on the observed spectrum of the XUV radiation [59, 73, 76].

A model for HHG was presented by Lewenstein et al [77] that put the quasi-classical behavior of the electron on firm footing starting out from the Schrödinger equation. Here, the time-dependent expectation value of the dipole moment at time t (and hence the source of radiation) is calculated by the integral over all previous times t':

$$x(t) = i\int dt' \int d^3\vec{p}\; \varepsilon \cos(t') d_x\left(\vec{p}+\vec{A}(t')\right) \times e^{-iS(\vec{p},t,t')} d_x^*\left(\vec{p}+\vec{A}(t)\right) + \text{c.c.} \qquad (12)$$

where d_x is the transition dipole moment to the continuum, d_x^* is the transition moment back down to the ground state, and the phase term in the middle contains the action S for

the electron's path through the continuum. $\vec{A}$ is the vector potential of the laser field and $\vec{p}$ is the canonical momentum. Of course, the electron can take any path, so we have to integrate over $\vec{p}$.

Let us have a closer look at the action. It is given by

$$S(\vec{p},t,t') = \int_{t'}^{t} dt'' \left(I_p + \frac{\left(\vec{p}+\vec{A}(t'')\right)^2}{2} \right). \qquad (13)$$

In a typical electron trajectory in HHG, the electron might return with 3 atomic units of energy (∼80 eV). The ionization potential, I_p, is typically half an a. u. and the time the electron spends in the continuum is the better portion of a laser cycle (∼80 atomic units of time, for an 800 nm laser pulse). Therefore the action can reach extremely large values compared to $\hbar$ and the stationary phase approximation is valid. That is to say, since we have to average over $\vec{p}$, only the trajectories near an extremum (typically a minimum) of the action need to be considered, while all the other ones cancel out due to the large phase variation upon slight changes to the non-stationary-phase trajectories. Therefore, we need to only count those trajectories that leave S at a minimum, $\delta S = 0$.

It is the validity of the stationary-phase approximation that marks the transition from quantum to classical Lagrangian mechanics. Effectively, a large action ensures that we can treat the particle as classical and the trajectory as classically "single" instead of quantum-mechanically "blurry". Thus the Lewenstein model puts on firm footing the already-successful three-step formulation of HHG, due originally to Corkum [50] and to Kulander [78], which is illustrated in Fig. 9. They argued that a semi-classical approach was sufficient to describe the salient points of HHG. After a quantum-mechanical "quasi-static" tunneling of a valence electron out from the atom, the electron would follow a classical trajectory influenced by the laser field and possibly recombine with its parent ion to emit a photon. This quasi-classical picture is also the reason that ATI can be understood in terms of classical trajectories: in ATI, the electron does not recombine with the ion (although it may scatter from the ion), but instead flies away into the continuum under the influence of the laser field.

With this understanding, we have the tools to choose driver pulse parameters (intensity, duration, polarization, CEP) *a priori* that lead to desired characteristics in the HHG spectra and ultimately to isolated attosecond pulses.

As an example of such choice, suppose we wish to make an isolated attosecond pulse with the simplest possible scheme: just make the driver pulse shorter and shorter until a sub-femtosecond XUV pulse is obtained. If a short driving pulse is used for HHG, the highest energy photons are released at the end of the half cycle with highest field strength – or, highest kinetic energy of the returning electron. In that case, the available bandwidth for the isolated attosecond pulse is given by the difference in return energies for electrons originating in the strongest cycle of the driver pulse and electrons originating in the second strongest.

Since the evolution of the driver pulse field during the electron propagation controls the return energy of the electron, the bandwidth requirement places a restriction on the duration of the driver pulse. Figure 10 shows the maximum allowable driver pulse duration as a function of peak intensity of the driver pulse, assuming the production of a 1 fs XUV pulse, the threshold of the attosecond regime. Intersections of dashed lines with the curves in the figure represent

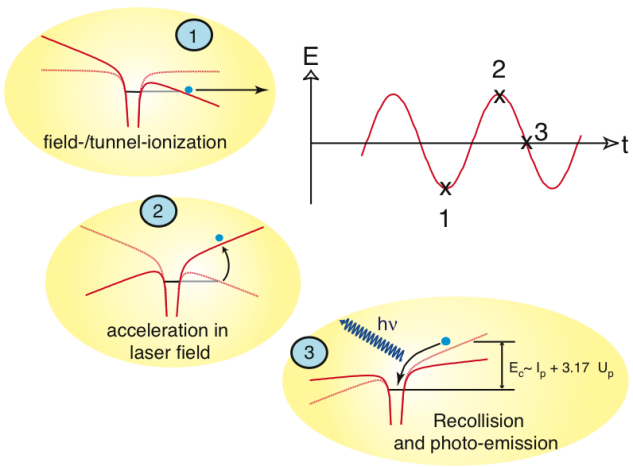

Figure 9 (online color at: www.lpr-journal.org) Quasi-classical model of high-harmonic generation [50, 78]. When an atom is exposed to a strong laser field, the Coulomb potential can be distorted so much that an electron can tunnel out into the continuum at time 1. Freed from the ion core, the electron follows the laser field according to Newton's equations, turning around at time 2. Finally, the electron has a chance to recombine with the ion at time 3, which leads to high-frequency photon emission.

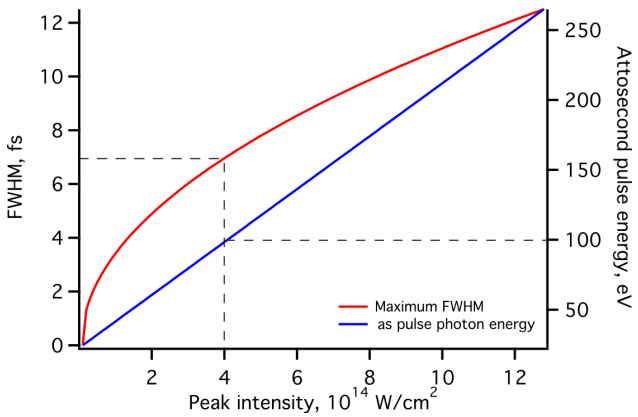

Figure 10 (online color at: www.lpr-journal.org) Constraints for sub-fs x-ray pulse production using the intensity variation at the peak of a short 800 nm driver pulse. Calculated pulse duration required to provide a 1 fs x-ray pulse as a function of intensity (light grey, red online), and calculated attosecond pulse photon energy as a function of intensity (dark grey, blue online). Intersections of dashed lines with the curves represent laser pulse parameters close to those used in some of the early attosecond pulse generation experiments [79, 80].

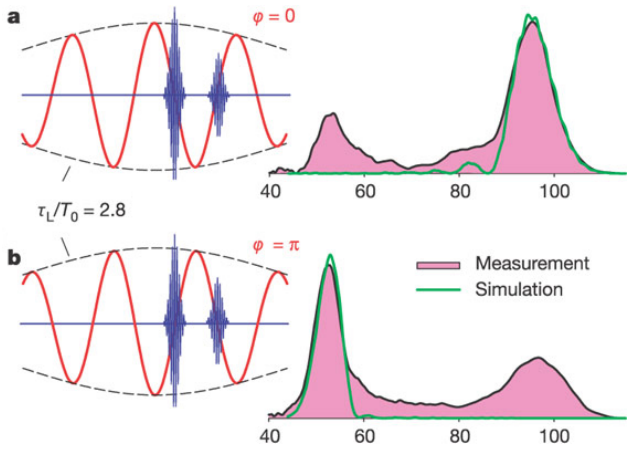

Figure 11 (online color at: www.lpr-journal.org) CEP-dependent attosecond double pulse. Experimental measurements from [59] which show the streaked photoelectron spectrum of an attosecond double pulse as a function of CEP. Photoelectrons generated by one attosecond pulse gain energy from the streaking laser field, while those from the second attosecond pulse lose energy to the field (for more details see [59,76]). The duration of the driving laser pulse τ_L is 2.8 times the carrier wave period T_0. The double-pulse contrast is controlled by the CEP.

the laser pulse parameters similar to those used in some of the early attosecond pulse generation experiments [79, 80].

At a given intensity and duration of the driver pulse, the CEP influences the difference in field strength between half cycles of the driver. Rotating the CEP can result in a pulse with either two identical half cycles or in one stronger half cycle (CEP zero). One can, therefore, obtain attosecond pulse pairs with variable, CEP-dependent contrast [59, 73, 81]. CEP-based control and optimization of the contrast has also been discussed in detail by the authors [76].

When an attosecond double pulse is emitted, the two pulses are separated in time by half a laser cycle. Overlapping these pulses with the (still synchronized) intense driver pulse in an atomic gas yields a photoelectron spectrum with each photoelectron line split into two: one peak is shifted to higher energy and one peak is shifted to lower energy. This is because the attosecond bursts come at the zero-crossings of the electric field, where the vector potential is extremized. One XUV pulse overlaps in time with a positive extreme of the vector potential, the other with a negative extreme [59, 76]. These photoelectrons, generated only half a laser cycle apart, are classically accelerated in opposite directions by the laser field. Figure 11 shows how the relative number of up- and down-shifted photoelectrons yields the contrast of the attosecond double pulse.

An interesting verification of the classical nature of the electron wavepackets' motion through the continuum is the phenomenon of half-cycle cutoffs (HCOs) [82, 83]. When phase matching conditions are set properly, the harmonic radiation emitted with low divergence can have enhanced emission at the cutoff frequency – the maximum photon energy classically allowed by the 3-step model [50]. Local maxima in the combined harmonic spectra therefore relate to the individual cutoff frequencies corresponding to each half-cycle of the driving laser field. This concept is illustrated in Fig. 12. By recording the harmonic spectrum in the HCO phase-matching regime as a function of CEP, one can use CEP control over the electron trajectories to map out the electric field strength of the laser pulse as a function of time [73, 84, 85].

In Fig. 13, the HHG spectra measured in Berkeley for a few-cycle pulse are plotted along with the HCO positions. The energy of the HCO allows access – through Newtonian mechanics – to the instantaneous value of the electric field during the electrons' excursion in the continuum. By varying

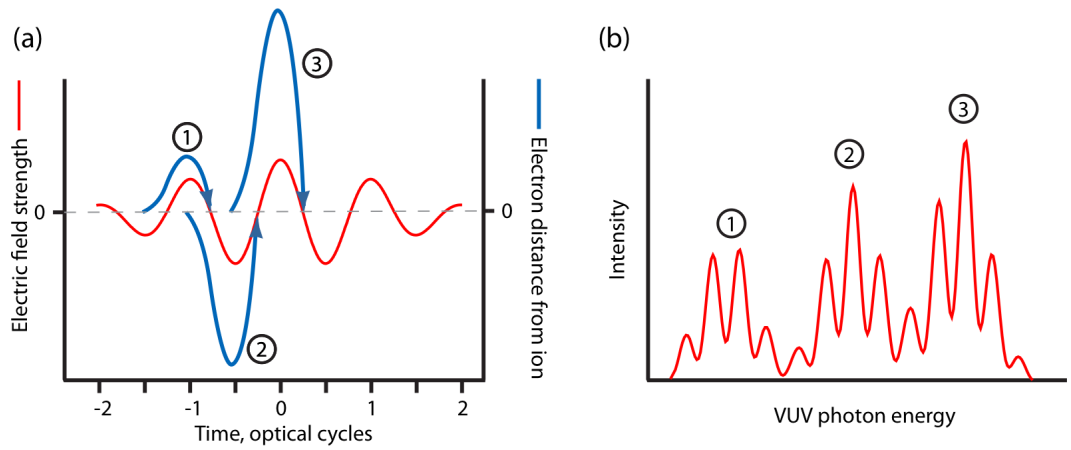

Figure 12 (online color at: www.lpr-journal.org) The origin of half-cycle cutoffs in harmonic generation, following the illustration from [82]. During each successive half cycle of the driving laser pulse, electrons tunnel out of the atom and travel through the continuum. Their classical trajectories are fully determined by the (CEP-dependent) sub-cycle evolution of the laser field to which they are exposed. Upon recollision, the cutoff harmonics (those photons with the highest kinetic energy allowed by classical mechanics) generated within each half cycle are preferentially phase-matched. Plot (a) shows the driving field and three electron trajectories leaving the ion at different times. Plot (b) shows how the harmonic emission for each half-cycle trajectory contributes to the overall (coherently summed) harmonic spectrum. Even in the full spectrum, the half-cycle cutoff energy positions are visible as local maxima of the harmonic spectrum.

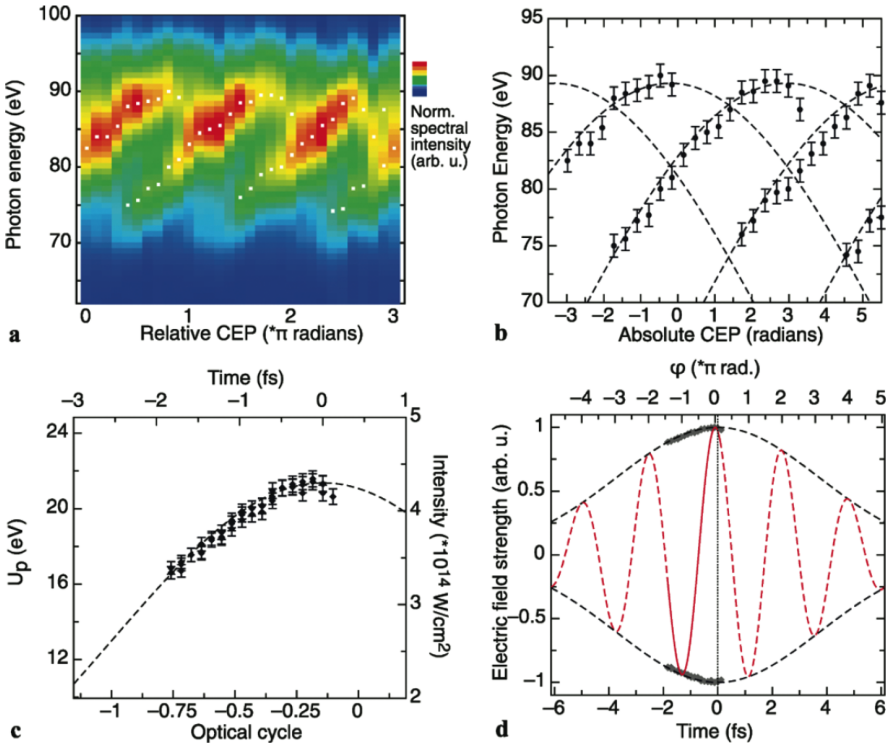

Figure 13 (online color at: www.lpr-journal.org) HCO positions as a function of CEP reveal the shape of the driving pulse, as reconstructed in [84]. Panel (a) shows experimental HCO spectra versus CEP offset with HCO positions marked. Panel (b) shows the HCO positions and Gaussian fits. Panel (c) is the same as Panel (b) but with the CEP (mod π) converted to optical cycles. Panel (d) shows the reconstructed few-cycle pulse.

the CEP, the times of electron emission and recollision are changed in a predictable way, and therefore the recollision energies (HCO positions) yield the driver pulse shape.

This is not the only example of CEP-based control in HHG. CEP-based control of electron trajectories was investigated by Sansone et al. [86] and by Nisoli et al. [87] in single-shot HHG experiments, and analyzed in similar Feynman path integral-like terms. All the isolated attosecond pulse production schemes so far discussed in the literature – intensity gating [3, 81, 88], polarization gating [89], two-color techniques [90–92], double optical gating [74, 93] – use the CEP to control the trajectories of electrons generated at different times in the driver laser pulse. In these techniques, the CEP determines whether electrons emitted from the atom during a temporal gate return to the ion to emit attosecond radiation. This concept of control by classical mechanics can be extended to CEP-based wavelength control over the emitted harmonic radiation [73, 84, 85]. By generating attosecond pulses on the leading edge of a driver pulse as discussed in [84, 85], an isolated attosecond pulse with tunable wavelength can also be obtained [85]. One simply has to separate the HCO emission events sufficiently in the frequency domain that only a single attosecond burst passes a high-pass filter (typically a thin metal foil) no matter what the CEP value is set to. Tuning the CEP, and thereby tuning the recolliding electron's kinetic energy, tunes the central wavelength of the emitted isolated attosecond pulse.

7. Summary

The CEP of short laser pulses offers a unique tool for control of electronic processes. We have reviewed different examples of control, all based on the interference of quantum pathways. In some cases the interfering pathways are a few countable ones in number; in this case, the term "quantum control", in its traditional meaning, is most applicable. In other cases, there are many such interfering pathways (typically when a continuum is involved), and interference among them often leads to the survival of only the shortest one, the classical trajectory. However, in both cases, the quantum and the classical mechanism, the CEP of strong-field laser pulses is an ideal parameter to steer electrons among different quantum states.

When the laser field is rather weak, i. e. in the (even multiple-order) perturbative limit, it can induce multiphoton transitions of differing order, ending in a common final state. The relative phase between these few transitions gives the final-state population. This scheme has long been used for separate phase-locked laser pulses; the CEP makes intra-pulse control available in the same way, due to its ultimately coherent nature and fully defined spectral phase.

Continuing in that spirit, we examined electron localization in dissociative ionization of molecules. Here as well, interference between nuclear wavepackets propagating on different electronic states and their potential curves with the same asymptotic energy leads to a spatial localization of the electron in the dissociation of diatomic cations. The relative populations and phases on the two curves can be tuned by changing the CEP of the laser, leading to a controllable asymmetry of electron localization. This is, of course, also few-path quantum interference. It remains an open question whether, also in the case of molecular control, it may finally be possible to classically control electron motion. This would allow fascinating perspectives, such as literally moving electrons from one bond to another one within mol-

ecules, mediated by fully coherent and extremely broadband CEP-stable light fields.

Finally, if the laser field is very strong, it can tunnel-ionize an atom or molecule. The continuum electron "feels" only the strong laser field and is accelerated classically. We can view the probability of return to the ion as a limiting case of quantum-path interference, where the excursions into the vacuum are very long. They have enormous action integrals (phases) associated with them, and therefore trajectories away from the minimal action path interfere destructively. This leads to the stationary-phase approximation, and the key to understanding how a quantum system like an electron/ion pair can act classically. Integrating Newton's equations then yields the trajectory of the quasi-classical particle and the experimentalist can control this trajectory by applying the appropriate force (electric field), which in turn is facilitated by the perfectly defined electric field of CEP-stabilized laser pulses.

From here, the field of ultrafast control – and of ultrafast physics in general – has many interesting avenues open ahead. From one point of view, CEP control is a key enabling technology for future experiments. It has opened the door to sub-fs XUV pulses for tracking atomic and molecular dynamics on the attosecond timescale. This is a breakthrough in ultrafast physics that is still in its infancy – very few groups around the world have as yet reported the measurement of attosecond light pulses, let alone applied them to the study of quantum systems. And yet, as has been noted in many other articles and reviews [3–5], attosecond spectroscopy holds the promise of revealing the fastest chemical and atomic events. It could, for example, reveal time-dependent electronic correlations, resolve the creation of important electronic states like excitons, or allow the study of nanoscopic electric fields [4, 68]. These diverse applications require robust and flexible attosecond sources, which in turn rely critically on the upstream laser sources. CEP stabilization thus becomes the cornerstone technology of future advances in ultrafast science.

In metrology too, direct synthesis and measurement of arbitrary frequencies is made possible in a compact and dramatically simplified manner via CEP-stabilized sources. Thus a parallel revolution to that of ultrafast science is on the verge in precision measurement science. A key challenge for the future of CEP science is to keep these two potentially divergent fields in close contact. While on the surface it may not seem that arbitrary frequency synthesis – for example – is relevant to the study of ultrafast processes, the lesson of the last two decades is clearly the opposite. When the beautifully precise control over electric fields achieved in the metrology community can be translated into precise control over electronic and nuclear wavefunctions, the ultrafast community will greatly benefit. The ability to make precision measurements with XUV sources [94–96] – relying as they do on the ultrafast process of high harmonic generation – will be one gift of ultrafast science to metrology.

In the future, it will also be very interesting to see how CEP-stabilized laser sources affect the field of quantum control. Ever since the invention of the laser, there has been interest in the using the light to direct the course of chemical reactions. Intensity, duration, and relative phase are all routinely used for control. But what advance will taming the CEP, the final free parameter of the laser pulse, bring? Since quantum control of chemical reactions is so similar to the control schemes laid out in this review, it is natural to expect that CEP-stabilization will also yield much stronger control over, and deeper insight into, light-driven chemical reactions. In particular, the ability to precisely control ionization and the classical path of particles in the continuum may be an important and interesting new tool for quantum control of chemical reactions.

The fundamental understanding of CEP effects in quantum control is a lesson that has been taught many times in physics before: choose a parameter that affects the phase of wavepackets traveling on separate quantum paths – when these wavepackets can be made to interfere, we gain control over the amplitude and therefore the outcome of the experiment. But only now it becomes possible to use man-made objects exhibiting perfect coherence on the time-scale of femtoseconds and attoseconds – CEP-controlled light fields – as tools to obtain comprehensive control of even such fundamental processes as electron motion in and around atoms and molecules. A multitude of scientific and technological advances can be expected from gaining such direct access to the ultimate building blocks of chemistry.

Acknowledgements. We acknowledge the MURI program of the Air Force Office of Scientific Research (AFOSR), contract FA9550-04-1-0242, and the National Science Foundation (NSF) Extreme Ultraviolet Center EEC-0310717 for their support of the Berkeley laboratory. Support is also acknowledged from National Science Foundation Chemistry grant CHE-0742662. The laboratory infrastructure and recent efforts are supported by the Director, Office of Science, Office of Basic Energy Sciences, of the U. S. Department of Energy under contract DE-AC02-05CH11231. T. P. acknowledges financial support by an MPRG grant of the Max-Planck-Gesellschaft.

Received: 3 September 2010, **Revised:** 19 November 2010, **Accepted:** 13 December 2010

Published online: 2 February 2011

Key words: Ultrafast laser science, laser control, attosecond physics.

Mark Abel earned his undergraduate degree in chemistry at Oregon State University, during which time he started his research career in coherent spectroscopy. He then moved to the University of California at Berkeley where he studied the production and measurement of attosecond light pulses. He earned his Ph. D. in 2010 under the direction of Professors Daniel Neumark and Stephen Leone with a thesis entitled "Attosecond X-ray Pulses for Molecular Electronic Dynamics". He is currently studying the cooling and trapping

of neutral molecules in the Molecular Physics Department of the Fritz Haber Institute in Berlin.

Daniel M. Neumark received his B. A. and an M. A. from Harvard University in 1977, and a Ph. D. in Physical Chemistry from the University of California, Berkeley, in 1984. Dr. Neumark is currently Professor and Chair in the Department of Chemistry, University of California, Berkeley, and is also a Faculty Senior Scientist at Lawrence Berkeley National Laboratory. His research interests include chemical dynamics and spectroscopy, with particular focus on transition state spectroscopy, high resolution photoelectron spectroscopy of negative ions, free radical photodissociation, cluster dynamics, electron solvation in liquid jets, and time-resolved experiments in the soft x-ray regime with femtosecond and attosecond light pulses.

Stephen R. Leone received his Ph. D. in Chemistry at the University of California at Berkeley in 1974. He held positions at the University of Southern California, at NIST and the University of Colorado. He was a Fellow and staff member of the National Institute of Standards and Technology as well as Adjoint Professor of Chemistry and Biochemistry and Lecturer of Physics at the University of Colorado. Since 2002 he is Professor of Chemistry and Physics at the University of California, Berkeley and Director of the Chemical Sciences Division and Chemical Dynamics Beamline at Lawrence Berkeley National Laboratory. His research interests include ultrafast laser investigations and soft x-ray probing of valence and core levels, attosecond physics and chemistry, state-resolved collision processes and kinetics investigations, nanoparticle fluorescence intermittency, aerosol chemistry and dynamics, probing with near field optical microscopy, and neutrals imaging.

Thomas Pfeifer received his M. A. in Physics at the University of Texas, Austin in 2000 and his Ph. D. in Physics at the University of Würzburg, Germany in 2004. From 2005-2008 he was a postdoctoral researcher in the Departments of Physics and Chemistry at the University of California, Berkeley, designing and setting up attosecond dynamics labs and performing experiments at Lawrence Berkeley National Laboratory. He is currently leader of the independent Max-Planck Research Group at MPIK in Heidelberg, Germany. His research interests include ultrafast (attosecond/femtosecond) lasers and spectroscopy of quantum dynamics, with particular emphasis on the study of electron motion and localization in atoms and molecules, strong-field physics, laser pulse shaping, electronic quantum interference and quantum control.

References

[1] M. Shapiro and P. Brumer, Rep. Progr. Phys. **66**, 859 (2003).
[2] G. Gerber and T. Brixner, Chem. Phys. Chem. **4**, 418 (2003).
[3] P. B. Corkum and F. Krausz, Nature Phys. **3**, 381 (2007).
[4] T. Pfeifer, M. J. Abel, P. M. Nagel, A. Jullien, Z. H. Loh, M. J. Bell, D. M. Neumark, and S. R. Leone, Chem. Phys. Lett. **463**, 11 (2008).
[5] F. Krausz and M. Ivanov, Rev. Mod. Phys. **81**, 163 (2009).
[6] D. J. Jones, S. A. Diddams, J. K. Ranka, A. Stentz, R. S. Windeler, J. L. Hall, and S. T. Cundiff, Science **288**, 635 (2000).
[7] H. R. Telle, G. Steinmeyer, A. E. Dunlop, J. Stenger, D. H. Sutter, and U. Keller, Appl. Phys. B **69**, 327 (1999).
[8] A. Apolonski, A. Poppe, G. Tempea, C. Spielmann, T. Udem, R. Holzwarth, T. Hänsch, and F. Krausz, Phys. Rev. Lett. **85**, 740 (2000).
[9] R. J. Jones, J. Diels, J. Jasapara, and W. Rudolph, Opt. Commun. **175**, 409 (2000).
[10] A. Baltuška, M. Uiberacker, E. Goulielmakis, R. Kienberger, V. Yakovlev, T. Udem, T. Hänsch, and F. Krausz, IEEE J. Sel. Top. Quantum Electron. **9**, 972 (2003).
[11] T. Fuji, J. Rauschenberger, C. Gohle, A. Apolonski, T. Udem, V. Yakovlev, G. Tempea, T. Hänsch, and F. Krausz, New J. Phys. **7**, 116 (2005).
[12] T. Fortier, D. Jones, J. Ye, S. Cundiff, and R. Windeler, Opt. Lett. **27**, 1436 (2002).
[13] T. Fortier, D. Jones, and S. Cundiff, Opt. Lett. **28**, 2198 (2003).
[14] D. J. Jones, S. A. Diddams, J. K. Ranka, A. Stentz, R. S. Windeler, J. L. Hall, and S. T. Cundiff, Science **288**, 635 (2000).
[15] S. Koke, C. Grebing, H. Frei, A. Anderson, A. Assion, and G. Steinmeyer, Nature Photon. **4**, 462 (2010).
[16] M. Kakehata, H. Takada, Y. Kobayashi, K. Torizuka, Y. Fujihira, T. Homma, and H. Takahashi, Opt. Lett. **26**, 1436 (2001).
[17] T. Hänsch, Chem. Phys. Chem. **7**, 1170 (2006).
[18] S. T. Cundiff and J. Ye, Rev. Mod. Phys. **75**, 325 (2003).
[19] T. Udem, R. Holzwarth, and T. Hänsch, Eur. Phys. J. - Spec. Top. **172**, 69 (2009).
[20] T. Fuji, J. Rauschenberger, A. Apolonski, V. Yakolev, G. Tempea, T. Udem, C. Gohle, T. Hänsch, W. Lehnert, M. Scherer, and F. Krausz, Opt. Lett. **30**, 332 (2005).
[21] D. J. Tannor and S. A. Rice, J. Chem. Phys. **83**, 5013 (1985).
[22] D. J. Tannor, R. Kosloff, and S. A. Rice, J. Chem. Phys. **85**, 5805 (1986).
[23] K. Bergmann, H. Theuer, and B. W. Shore, Rev. Mod. Phys. **70**, 1003 (1998).
[24] M. Shapiro, J. W. Hepburn, and P. Brumer, Chem. Phys. Lett. **149**, 451 (1988).
[25] P. Brumer and M. Shapiro, Chem. Phys. Lett. **126**, 541 (1986).
[26] M. Shapiro, J. Hepburn, and P. Brumer, Chem. Phys. Lett. **149**, 451 (1988).
[27] G. G. Paulus, F. Grasbon, H. Walther, P. Villoresi, M. Nisoli, S. Stagira, E. Priori, and S. D. Silvestri, Nature **414**, 182 (2001).
[28] T. Nakajima and S. Watanabe, Phys. Rev. Lett. **96**, 213001 (2006).
[29] T. Nakajima and S. Watanabe, Opt. Lett. **31**, 1920 (2006).
[30] T. Fortier, P. Roos, D. Jones, S. Cundiff, R. Bhat, and J. Sipe, Phys. Rev. Lett. **92**, 147403 (2004).

[31] P. A. Roos, X. Li, R. P. Smith, J. A. Pipis, T. M. Fortier, and S. T. Cundiff, Opt. Lett. **30**, 735 (2005).
[32] E. Dupont, P. B. Corkum, H. C. Liu, M. Buchanan, and Z. R. Wasilewski, Phys. Rev. Lett. **74**, 3596 (1995).
[33] V. Roudnev and B. D. Esry, Phys. Rev. Lett. **99**, 220406 (2007).
[34] A. Giusti-Suzor, F. H. Mies, L. F. DiMauro, E. Charron, and B. Yang, J. Phys. B, At. Mol. Opt. Phys. **28**, 309 (1995).
[35] J. Posthumus, Rep. Prog. Phys. **67**, 623 (2004).
[36] V. Roudnev, B. Esry, and I. Ben-Itzhak, Phys. Rev. Lett. **93**, 1 (2004).
[37] A. Bandrauk, S. Chelkowski, and H. Nguyen, Int. J. Quant. Chem. **100**, 834 (2004).
[38] M. F. Kling, C. Siedschlag, A. J. Verhoef, J. I. Khan, M. Schultze, T. Uphues, Y. Ni, M. Uiberacker, M. Drescher, F. Krausz, and M. J. J. Vrakking, Science **312**, 246 (2006).
[39] A. V. Davis, R. Wester, A. E. Bragg, and D. M. Neumark, J. Chem. Phys. **118**, 999 (2003).
[40] R. Mabbs, K. Pichugin, and A. Sanov, J. Chem. Phys. **123**, 054329 (2005).
[41] M. V. Ammosov, N. B. Delone, and V. P. Krainov, Sov. Phys. JETP **64**, 1191 (1986).
[42] G. L. Yudin and M. Y. Ivanov, Phys. Rev. A **64** (2001).
[43] M. Kremer, B. Fischer, B. Feuerstein, V. L. B. de Jesus, V. Sharma, C. Hofrichter, A. Rudenko, U. Thumm, C. D. Schroter, R. Moshammer, and J. Ullrich, Phys. Rev. Lett. **103**, 213003 (2009).
[44] I. Znakovskaya, P. von den Hoff, S. Zherebtsov, A. Wirth, O. Herrwerth, M. J. J. Vrakking, R. de Vivie-Riedle, and M. F. Kling, Phys. Rev. Lett. **103**, 103002 (2009).
[45] G. Sansone, F. Kelkensberg, J. F. Pérez-Torres, F. Morales, M. F. Kling, W. Siu, O. Ghafur, P. Johnsson, M. Swoboda, E. Benedetti, F. Ferrari, F. Lépine, J. L. Sanz-Vicario, S. Zherebtsov, I. Znakovskaya, A. L'Huillier, M. Y. Ivanov, M. Nisoli, F. Martín, and M. J. J. Vrakking, Nature **465**, 763 (2010).
[46] F. Kelkensberg, C. Lefebvre, W. Siu, O. Ghafur, T. Nguyen-Dang, O. Atabek, A. Keller, V. Serov, P. Johnsson, M. Swoboda, T. Remetter, A. L'Huillier, S. Zherebtsov, G. Sansone, E. Benedetti, F. Ferrari, M. Nisoli, F. Lépine, M. Kling, and M. Vrakking, Phys. Rev. Lett. **103**, 1 (2009).
[47] W. Becker, A. Lohr, and M. Kleber, Quantum Semiclassical Opt. **7**, 423 (1995).
[48] K. Burnett, V. Reed, and P. Knight, J. Phys. B, At. Mol. Opt. Phys. **26**, 561 (1993).
[49] S. Augst, D. D. Meyerhofer, D. Strickland, and S. L. Chin, J. Opt. Soc. Am. B **8**, 858 (1991).
[50] P. Corkum, Phys. Rev. Lett. **71**, 1994 (1993).
[51] E. Cormier and P. Lambropolous, Eur. Phys. J. D **2**, 15 (1998).
[52] A. J. Verhoef, A. Fernandez, M. Lezius, K. O'Keeffe, M. Uiberacker, and F. Krausz, Opt. Lett. **31**, 3520 (2006).
[53] D. B. Milošević, G. G. Paulus, and W. Becker, Laser Phys. Lett. **1**, 93 (2004).
[54] M. J. Abel, T. Pfeifer, A. Jullien, P. M. Nagel, M. J. Bell, D. M. Neumark, and S. R. Leone, J. Phys. B, At. Mol. Opt. Phys. **42**, 075601 (2009).
[55] G. G. Paulus, F. Lindner, H. Walther, A. Baltuška, E. Goulielmakis, M. Lezius, and F. Krausz, Phys. Rev. Lett. **91**, 253004 (2003).
[56] M. F. Kling, J. Rauschenberger, A. J. Verhoef, E. Hasovic, T. Uphues, D. B. Milošević, H. G. Muller, and M. J. J. Vrakking, New J. Phys. **10**, 025024 (2008).
[57] P. Colosimo, G. Doumy, C. I. Blaga, J. Wheeler, C. Hauri, F. Catoire, J. Tate, R. Chirla, A. M. March, G. G. Paulus, H. G. Muller, P. Agostini, and L. F. Dimauro, Nature Phys. **4**, 386 (2008).
[58] E. Constant, V. Taranukhin, A. Stolow, and P. Corkum, Phys. Rev. A **56**, 3870 (1997).
[59] R. Kienberger, E. Goulielmakis, M. Uiberacker, A. Baltuška, V. Yakovlev, F. Bammer, A. Scrinzi, T. Westerwalbesloh, U. Kleineberg, U. Heinzmann, M. Drescher, and F. Krausz, Nature **427**, 817 (2004).
[60] M. G. Schätzel, F. Lindner, G. G. Paulus, H. Walther, E. Goulielmakis, A. Baltuška, M. Lezius, and F. Krausz, Appl. Phys. B **79**, 1021 (2004).
[61] T. Wittmann, B. Horvath, W. Helml, M. G. Schatzel, X. Gu, A. L. Cavalieri, G. G. Paulus, and R. Kienberger, Nature Phys. **5**, 357 (2009).
[62] A. Staudte, D. Pavicic, S. Chelkowski, D. Zeidler, M. Meckel, H. Niikura, M. Schoffler, B. Ulrich, P. P. Rajeev, T. Weber, T. Jahnke, D. M. Villeneuve, A. D. Bandrauk, C. L. Cocke, P. B. Corkum, and R. Dorner, Phys. Rev. Lett. **98** (2007).
[63] S. Micheau, Z. Chen, A. Le, J. Rauschenberger, M. Kling, and C. Lin, Phys. Rev. Lett. **102**, 1 (2009).
[64] M. Meckel, D. Comtois, D. Zeidler, A. Staudte, D. Pavicic, H. C. Bandulet, H. Pepin, J. C. Kieffer, R. Dorner, D. M. Villeneuve, and P. B. Corkum, Science **320**, 1478 (2008).
[65] A. Becker and F. H. M. Faisal, J. Phys. B, At. Mol. Opt. Phys. **38**, R1 (2005).
[66] V. S. Popov, Phys. - Usp. **47**, 855 (2004).
[67] H. R. Reiss, Phys. Rev. A **22**, 1786 (1980).
[68] M. I. Stockman, M. F. Kling, U. Kleineberg, and F. Krausz, Nature Photon. **1**, 539 (2007).
[69] L. Pan, K. Taylor, and C. Clark, J. Opt. Soc. Am. B **7**, 509 (1990).
[70] L. Pan, K. Taylor, and C. Clark, Phys. Rev. A **39**, 4894 (1989).
[71] G. Farkas and C. Toth, Phys. Lett. A **168**, 447 (1992).
[72] G. Sansone, E. Benedetti, F. Calegari, C. Vozzi, L. Avaldi, R. Flammini, L. Poletto, P. Villoresi, C. Altucci, R. Velotta, S. Stagira, S. D. Silvestri, and M. Nisoli, Science **314**, 443 (2006).
[73] M. J. Abel, T. Pfeifer, P. M. Nagel, W. Boutu, M. J. Bell, C. P. Steiner, D. M. Neumark, and S. R. Leone, Chem. Phys. **366**, 9 (2009).
[74] H. Mashiko, S. Gilbertson, C. Li, S. D. Khan, M. M. Shakya, E. Moon, and Z. Chang, Phys. Rev. Lett. **100**, 103906 (2008).
[75] I. Thomann, A. Bahabad, X. Liu, R. Trebino, M. Murnane, and H. Kapteyn, Opt. Express **17**, 4611 (2009).
[76] T. Pfeifer, M. Abel, P. Nagel, W. Boutu, M. Bell, Y. Liu, D. Neumark, and S. Leone, Opt. Lett. **34**, 1819 (2009).
[77] M. Lewenstein, P. Balcou, M. Ivanov, A. L'Huillier, and P. Corkum, Phys. Rev. A **49**, 2117 (1994).
[78] K. C. Kulander, K. J. Schafer, and J. L. Krause, in: Proceedings of the Workshop on Super-Intense Laser Atom Physics (SILAP) III, edited by B. Piraux (Plenum Press, New York, 1993), p. 95.
[79] R. Kienberger, E. Goulielmakis, M. Uiberacker, A. Baltuška, V. Yakovlev, F. Bammer, A. Scrinzi, T. Westerwalbesloh, U. Kleineberg, U. Heinzmann, M. Drescher, and F. Krausz, Nature **427**, 817 (2004).

[80] M. Drescher, M. Hentschel, R. Kienberger, M. Uiberacker, V. Yakovlev, A. Scrinzi, T. Westerwalbesloh, U. Kleineberg, U. Heinzmann, and F. Krausz, Nature **419**, 803 (2002).
[81] E. Goulielmakis, M. Schultze, M. Hofstetter, V. S. Yakovlev, J. Gagnon, M. Uiberacker, A. L. Aquila, E. M. Gullikson, D. T. Attwood, R. Kienberger, F. Krausz, and U. Kleineberg, Science **320**, 1614 (2008).
[82] C. A. Haworth, L. E. Chipperfield, J. S. Robinson, P. L. Knight, J. P. Marangos, and J. W. G. Tisch, Nature Phys. **3**, 52 (2007).
[83] L. Chipperfield, J. Robinson, P. Knight, J. Marangos, and J. Tisch, Laser Photonics Rev. **4**, 697 (2010).
[84] A. Jullien, T. Pfeifer, M. J. Abel, P. M. Nagel, M. J. Bell, D. M. Neumark, and S. R. Leone, Appl. Phys. B, Lasers Opt. **93**, 433 (2008).
[85] T. Pfeifer, A. Jullien, M. J. Abel, P. M. Nagel, L. Gallmann, D. M. Neumark, and S. R. Leone, Opt. Express **15**, 17120 (2007).
[86] G. Sansone, C. Vozzi, S. Stagira, M. Pascolini, L. Poletto, P. Villoresi, G. Tondello, S. D. Silvestri, and M. Nisoli, Phys. Rev. Lett. **92**, 1 (2004).
[87] M. Nisoli, G. Sansone, S. Stagira, S. D. Silvestri, C. Vozzi, M. Pascolini, L. Poletto, P. Villoresi, and G. Tondello, Phys. Rev. Lett. **91**, 1 (2003).
[88] M. Hentschel, R. Kienberger, C. Spielmann, G. A. Reider, N. Milosevic, T. Brabec, P. Corkum, U. Heinzmann, M. Drescher, and F. Krausz, Nature **414**, 509 (2001).
[89] G. Sansone, E. Benedetti, F. Calegari, C. Vozzi, L. Avaldi, R. Flammini, L. Poletto, P. Villoresi, C. Altucci, R. Velotta, S. Stagira, S. D. Silvestri, and M. Nisoli, Science **314**, 443 446 (2006).
[90] T. Pfeifer, L. Gallmann, M. J. Abel, P. M. Nagel, D. M. Neumark, and S. R. Leone, Phys. Rev. Lett. **97**, 163901 (2006).
[91] T. Pfeifer, L. Gallmann, M. J. Abel, D. M. Neumark, and S. R. Leone, Opt. Lett. **31**, 975 (2006).
[92] H. Merdji, T. Auguste, W. Boutu, J. P. Caumes, B. Carre, T. Pfeifer, A. Jullien, D. M. Neumark, and S. R. Leone, Opt. Lett. **32**, 3134 (2007).
[93] H. Mashiko, S. Gilbertson, C. Li, E. Moon, and Z. Chang, Phys. Rev. A **77**, 063423 (2008).
[94] M. Herrmann, M. Haas, U. Jentschura, F. Kottmann, D. Leibfried, G. Saathoff, C. Gohle, A. Ozawa, V. Batteiger, S. Knünz, N. Kolachevsky, H. Schüssler, T. Hänsch, and T. Udem, Phys. Rev. A **79**, 1 (2009).
[95] D. Kandula, C. Gohle, T. Pinkert, W. Ubachs, and K. Eikema, Phys. Lett. Lett. **105**, 1 (2010).
[96] D. C. Yost, T. R. Schibli, and J. Ye, Opt. Lett. **33**, 1099 (2008).